Hierarchically Ordered Polymer Nanofibers via Electrospinning and Controlled Polymer Crystallization

Bingbing Wang, Bing Li, Jie Xiong,[†] and Christopher Y. Li*

A. J. Drexel Nanotechnology Institute and Department of Materials Science and Engineering, Drexel University, Philadelphia, Pennsylvania 19104

Received August 30, 2008
Revised Manuscript Received October 30, 2008

Introduction. Electrospinning has recently attracted great attention in the field of material science and nanotechnology.[1−7] Uniform and/or functional nanofibers of polymers and inorganic materials as well as their hybrid composites have been formed either by direct electrospinning polymer solution/melt or by surface decorating the preformed nanofibers.[4,8] The high specific surface area associated with the nanofiber morphology holds the promise of using these nanofibers for a variety of applications. With the development of numerous novel electrospinning techniques, such as bicomponent,[9−11] coaxial and two-flow/phase,[12−15] and layer-by-layer electrospinning,[16] great successes have been achieved in controlling the surface morphology,[17−21] inner fiber phase separation,[22,23] and spatial alignment of the nanofibers.[24−27] Recently, the research focus in this field has gradually shifted from optimizing electrospinning conditions to investigating complex nanofiber structures (core/sheath, hollow, and porous structures) and to developing hybrid, hierarchical, and multifunctional structures in order to realize their potential applications in the fields of drug delivery,[28,29] sensors,[30−32] catalyst support,[33−35] and tissue engineering.[36−41] In particular, hybrid systems with the combination of nanoparticles and polymer nanofibers grant the latter with multifunctionality, leading to possible applications in photoelectronic devices.[42−49] Hierarchically ordered nanofibers have been achieved by introducing block copolymers into the systems, either as the fiber materials or as the component that is confined in the nanotubular structure created by coaxial electrospin.[22,50−52] Features at different length scales have also been introduced to the nanofiber systems using a secondary deposition technique. For example, Rutledge et al. reported the formation of hierarchically roughened nonwoven fabrics by decorating electrospun fibers (diameter ca. 1 μm) with pores or particles; the resultant nanofiber mats exhibited an interesting superhydrophobic behavior.[53,54] Superoleophobic surfaces based on nanofibers have also been observed.[55] Herein, we report a novel method of fabricating hierarchically ordered nanofibers by combining electrospinning and controlled polymer crystallization techniques. Polymer single crystals with tunable sizes were periodically grown on the electrospun nanofibers with a period of a few tens of nanometers. This unique nanoscale architecture can be used as the template to fabricate hybrid, multifunctional structures. As a proof-of-concept, we demonstrated that gold nanoparticles (AuNPs) could be periodically immobilized on the nanofiber surface. This hybrid structure may find applications as sensing or catalyst-supporting materials.

* Corresponding author: phone 215-895-2083; Fax 215-895-6760; e-mail Chrisli@drexel.edu.
[†] Current address: Key Laboratory of Advanced Textile Materials and Manufacturing Technology Ministry of Education, Zhejiang Sci-Tech University, Hangzhou, Zhejiang 310018, China.

Experimental Section. *Materials and Measurements.* Poly(ethylene oxide) (PEO, number-average molecular weight M_n = 300K g/mol), dimethylformamide (DMF, 99.8%±), toluene (99.5%±), gold(III) chloride (99%), tetrabutylammonium borohydride (98%), and didodecyldimethylammonium bromide (98%) were purchased from Aldrich and were used as received. Thiol-terminated poly(ethylene oxide) (HS-PEO, M_n = 2K g/mol) was purchased from Polymer Source. Gold nanoparticles (AuNPs) with the diameter of ∼6 nm were synthesized according to the literature.[56] Sodium periodate and ruthenium(IV) oxide hydrate were purchased from SPI Co.

Transmission electron microscopy (TEM) was carried out using a JEOL 2000FX TEM operating at an acceleration voltage of 120 kV. PEO nanofibers were electrospun onto the surface of a carbon-coated nickel TEM grid. After the formation of kebab crystals, the TEM grid was dried under vacuum and was used for TEM observation. Ruthenium tetroxide (RuO_4) was used to stain some of the TEM samples as indicated. Scanning electron microscopy (SEM) was carried out using an environmental SEM (FEI XL30) at an acceleration voltage of 10 kV. The SEM samples were prepared by electrospinning nanofibers on the surface of glass slides. After the formation of kebab crystals, the glass slides were dried under vacuum to remove excess solvents. Before SEM testing, platinum coating (30 s, 40 mA) was performed by using a Gressington sputter coater 208HR in order to increase the conductivity of the polymer nanofiber.

Electrospinning of Nanofibers. Nanofibers were electrospun from PEO/DMF solution which was formed by dissolving PEO at 65 °C for 30 min. The concentration was 9 wt % in order to avoid the bead formation during the electrospinning. The voltage and collecting distance were 25 kV and 15 cm, respectively. A piece of aluminum foil was used as the ground collector. Both TEM grids and glass slides were also used to collect the nanofibers for further tests.

Polymer Crystallization. (1) Crystallization by incubation: Polymer solutions were prepared from either 300K PEO or HS-PEO using DMF as the solvent. Electrospinning nanofibers of PEO, which were collected on the surface of glass slides and/or TEM grids, were incubated in a polymer solution for 60 min. The nanofibers were then taken out from the solution and washed with DMF to remove free polymers. Before other tests, the nanofibers were dried under vacuum for 24 h. *(2) Crystallization by solvent evaporation:* The PEO nanofibers were collected on the surface of TEM grids. 5 μL of polymer solution (2K HS-PEO with the concentration of 0.05 wt %) was drop-cast on the nanofibers and dried at room temperature.

AuNPs Immobilization on Nanofibers. AuNPs (diameter ∼6 nm) were synthesized as reported and were dispersed in toluene. HS-PEO decorated nanofibers were immersed in the AuNP solution for 60 min. Free AuNPs and ligands were removed by repeatedly washing with toluene.

Results and Discussion. PEO (M_n = 300K g/mol) nanofibers were obtained by electrospinning a PEO/DMF solution following the reported method.[57] Smooth fibers with a diameter of ∼200 nm were obtained as seen from the SEM image in Figure 1a. These nanofibers were then incubated in a 0.3 wt % PEO/DMF solution. After a certain crystallization time (∼60 min), these PEO molecules crystallized on the nanofiber surface, and the free polymers were removed by repeated washing. The

10.1021/ma801971r CCC: $40.75
Published on Web 11/14/2008

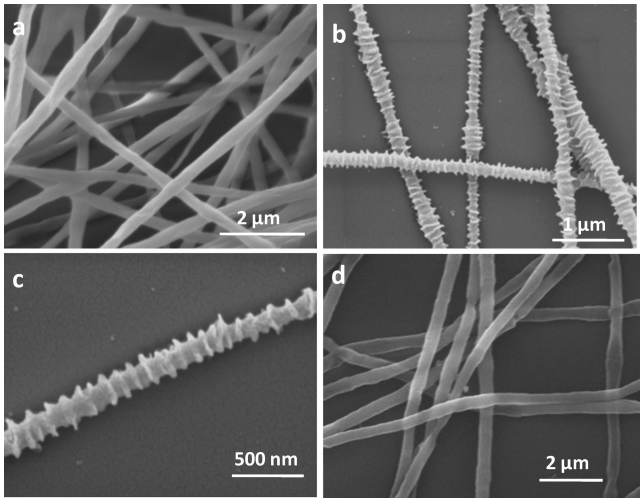

Figure 1. SEM images of electrospun PEO nanofibers (a) and NFSKs coated with 300K PEO as the K-P at a concentration of 0.3 wt % at low (b) and high magnifications (c). (d) shows a SEM images of PEO nanofibers incubated in pure DMF for 1 h.

remaining nanofibers were dried for 24 h at room temperature under vacuum. Figures 1b,c show SEM images of the resultant structure. After solution incubation, the original PEO nanofiber structures retained. On the surface of these nanofibers, a uniform decoration of edge-on PEO single crystals can be clearly seen. The crystals are relatively periodically located along the PEO nanofibers. This unique structure is apparently hierarchical as the nanofibers have the diameters on the ~200 nm scale, the crystals have a thickness of ~10−20 nm, and the period is ~90 nm. A control experiment was conducted by incubating PEO nanofibers in pure DMF for 60 min. No lamellar crystals were observed (Figure 1d), indicating that the formation of lamellar crystals on the surface of nanofibers was because that the secondary PEO crystallized onto the nanofiber surface.

Recently, we reported an approach of using the controlled solution crystallization method to periodically pattern polymers on carbon nanotubes (CNTs).[58−63] Similar results have also been observed by a few other groups.[64−66] Polymer single crystals were periodically decorated on CNTs, rendering a unique nanostructure named as nano hybrid shish kebab (NHSK), which mimics the conventional shish-kebab structure formed when polymers crystallize under an extensional field.[67] Both polyethylene and nylon-66 were used to form kebabs on CNTs. In NHSKs, CNTs serve as the 1-D shish while polymer single crystals are the kebabs. The structure in Figures 1b,c is similar to the NHSK we reported earlier. We thus name the present structure as nano fiber shish kebab (NFSK) because the central stem of this structure is a polymer nanofiber. Scheme 1 shows a schematic representation of the formation process of NFSK. We also coin the names S-P and K-P to stand for the shish-forming polymer and the kebab-forming polymer, respectively. Note that in NFSK, since the fiber diameter is relatively larger, the kebab crystal resembles a toroid structure with the central hole occupied by the nanofiber (Scheme 1). From Figure 1b, the central hole of the toroid is ~200 nm while the width of the toroids is ~30 nm. Compared with the previously reported NHSK, the present NFSK structure is more general because there are numerous types of polymers that can be electrospun into nanofibers to form NFSK, while in NHSK the shish is only formed by CNTs. As one example, the PEO NFSK is of great interest because PEO has found profound applications in many biological fields including biomedical, bioengineering, controlled drug release, etc. The immediate advantages of PEO NFSK are

Scheme 1. Schematic Representation of the Nano Fiber Shish Kebab

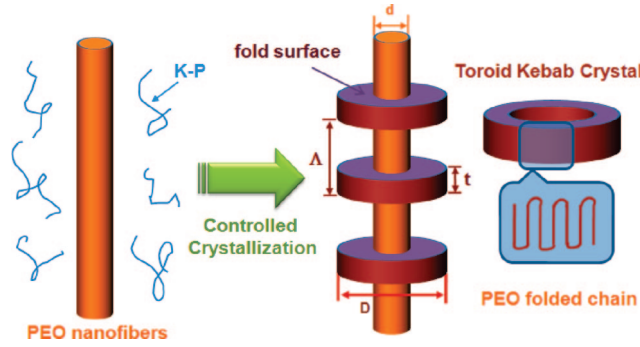

the following: First, the rationale of using nonwoven nanofiber mats for biomedical applications such as wound dressing is because the fiber mats are porous and/or biodegradable. However, the porosity of the mat is controlled only by the fiber diameter and the tunability is limited. Compared with a nonwoven nanofiber mat, a NFSK mat renders a 3-D feature to the 1-D nanofiber because the 2-D crystal lamellae are perpendicular to the nanofiber axis. This NFSK thus provides much higher specific surface areas compared with nanofibers. Furthermore, membranes made of these NFSK possess a more open structure because the kebabs serve as the spacers that keep the nanofibers apart, leading to a wider tuning window for the porosity control. Second, since forming NFSK is a two-step process, S-P and K-P in a NFSK could be the same/different polymers. Controlled biodegradation could be realized when two different polymers are used to form the shish and the kebab. This is of great interest from a tissue engineering viewpoint. Third, NFSK can also be used as the nanoscale template to immobilize nanoparticles/functional groups on the nanofiber surfaces in a controlled manner, leading to ordered multifunctional nanofibers (see later for examples). Polymer nanofibers and CNTs share the similarity that both objects are 1-D and the diameter ranges from a few tens to hundreds of nanometers. We have attempted to induce PEO crystallization using CNTs and our preliminary results suggested that PEO did not crystallize on pristine CNTs in a polymer solution crystallization process, possibly because of the unfavorable interaction between CNTs and the PEO chains. In the present case, compared with CNTs, PEO nanofibers are more compatible with free PEO chains in solution. The latter can thus easily absorb onto the nanofiber surface and crystallize. NFSK further confirms that the formation of the shish-kebab structure is a general feature for 1-D nanotube/nanofiber-induced crystal growth.

The unique NFSK can be easily tuned for the application purposes. We define a NFSK using a few parameters as shown in Scheme 1, namely the diameter of kebab D, the nanofiber diameter d, the lamellar thickness t, and the period Λ. All these parameters can be readily tuned. For instance, d can be controlled by electrospinning conditions such as the S-P concentration, electrospinning voltage, spinnerette-to-collector distance, etc. D, t, and Λ can be controlled by tuning the crystallization conditions such as crystallization time, temperature, the K-P concentration, M_n, etc. In our preliminary work, by simply changing K-P concentration from 0.06 to 0.8 wt %, both D and Λ changed significantly as shown in Figure 2. At low concentration (0.06 wt %), small polymer crystallites with a lateral dimension of ~20−30 nm randomly decorated on the fiber surface. These crystallites are separated from each other, and a complete toroid did not form as shown in Figure 2a. As the concentration increased, these discrete crystals connected

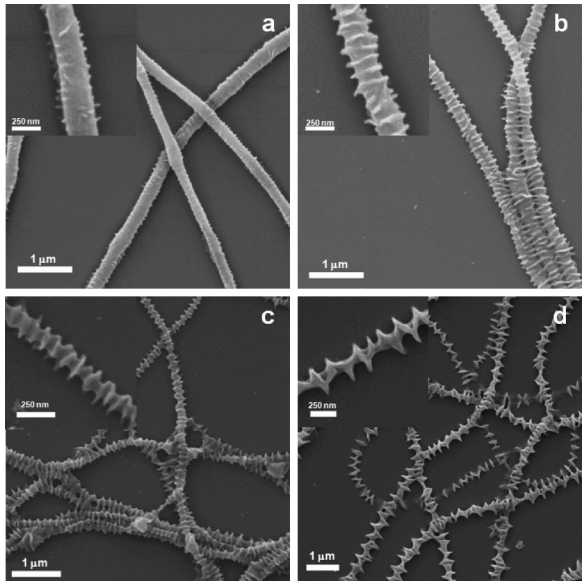

Figure 2. SEM images of NFSKs formed at different K-P polymer concentrations: 0.06 (a), 0.3 (b), 0.5 (c), and 0.8 wt % (d). Insets are enlarged images.

with each other, forming toroid around the underneath nanofiber. The toroid width [$(D - d)/2$] in Figure 2b is ~30 nm. The circumference of the kebabs is ~600−700 nm, and the period Λ is ~90 nm (Figure 2b). Further increasing K-P concentration led to the increase of both the kebab crystal size and the period Λ as revealed in Figure 2. Large kebabs with the toroid width of ~100−200 nm were obtained when the concentration of K-P increased to 0.8 wt % (Figure 2d). Increase of the kebab size is anticipated as the K-P concentration increases. However, increase of Λ is intriguing. In the present case, it is evident from the inset of Figure 2d that, as the kebab size increased, adjacent lamellae merged together. This is because polymer lamellae are relatively flexible. As the lamellar lateral size increased, during crystallization, the capillary force between the adjacent kebabs might have pulled the crystals together. Upon merging, the period Λ increased and the kebabs formed a zigzag pattern as shown in the inset of Figure 2d.

Also of interest is that, in the NFSK shown in Figures 1 and 2, all the kebabs are (or close to be) perpendicular to the nanofiber axis, indicating that the PEO chains in the kebab crystals are parallel to the fiber. We attribute this orientation to the soft epitaxy mechanism of the PEO kebab growth: in PEO nanofiber, the polymers are parallel to the fiber axis because of the chain stretching during the electrospinning process. As the PEO coil chains nucleate on the nanofiber surface, the chain tends to orient parallel to the fiber axis although a strict crystallography matching between the nanofiber and the kebabs may not be fulfilled. Note that this is similar to the classic polymer shish-kebab structures: because polymer chains have a uniaxial fiber orientation in the shish, while the kebabs are single-crystal lamellae, crystallographic lattice matching between the shish and the kebabs can, in the best scenario, only be fulfilled at a few local locations at the shish/kebabs interface. Hence, the overall relationship between the shish and the kebab is best described as the soft epitaxy. Figure 3 shows the electron diffraction patterns and the corresponding bright field TEM images of the PEO nanofiber (a, b) and NFSKs (c, d, e, f). Note that the diffraction in (c) was from both the shish and the kebab (d) while the diffraction in (e) was only from the kebab area (f). In all the three cases, the characteristic (120) diffraction of the PEO can be observed as arcs orientated perpendicular to the fiber axes, indicating that the PEO chains are parallel to the fibers and the kebab lamellar normal.[68,69] The hierarchical structure of the NSFK is shown in Scheme 1.

The unique NFSK architecture opens the gateway to synthesizing periodically patterned multifunctional nanofibers. To this end, end-functionalized polymers may be used to form the kebabs. Since the end functional groups are different from the rest of the polymer backbone, upon crystallization, they are normally excluded to the kebab crystal surface. The kebabs therefore can be used as a vehicle to introduce a variety of functional groups on the nanofibers. In our preliminary study, we used the NFSK to immobilize AuNPs. Research on fabricating nanoparticle/nanofiber hybrids has attracted great attention recently because the resultant 1-D hybrid structure could find numerous applications in nanoelectronics as well as biomedical fields. NPs have been coelectrospun with polymers, and they can also be formed after nanofiber formation.[43,47,70] Recently, we demonstrated that AuNPs could be immobilized on the surface of HS-PEO single crystals.[71−73] In the present study, we used HS-PEO (M_n ~2K g/mol) as the K-P to form the kebabs on the PEO nanofibers. Relatively low M_n polymer was used since it can be readily functionalized with a thiol group. Figure 4 shows the TEM images of HS-PEO NFSKs. The sample was stained using RuO_4 to enhance the contrast. Regular dark lines are clearly reviewed from the image. These lines run across the nanofiber, and they align perpendicular to the fiber axis. The lines are also periodically located along the nanofibers, and the period is ~20 nm. The dark lines are formed as a result of the preferred staining of RuO_4 near and/or at the surface of the edge-on HS-PEO single crystals. This is because that the surface has (1) the enrichment of the thiol groups and (2) relatively loosely packed EO units compared with the inner area of the crystal. The inset of Figure 4b shows the details of the molecular packing. The structure is slightly different from the NFSK in Figure 1. The previous toroids are not evident from Figure 4. Instead, the coating is relatively continuous. This can be attributed to the low polymer M_n of HS-PEO. Compared with the 300K PEO, 2K HS-PEO possesses a higher diffusion coefficient, which leads to a faster heterogeneous nucleation on the preformed nanofibers. Therefore, more continuous coating of PEO crystals was observed in 2K HS-PEO NFSKs.

We envisaged that this periodic enrichment of the thiol groups along the nanofibers could lead to controllable AuNP patterning. To this end, NFSKs were first formed by crystallizing 0.5 and 5 wt % 2K HS-PEO on 300K PEO nanofibers. These HS-PEO NFSKs were incubated with AuNP (6 nm in diameter) sol for 60 min. The NFSKs were then thoroughly rinsed with toluene to remove free ligands and AuNPs. Figures 5a,b show the TEM images of the resultant structure. Note that the NFSKs in both figures were not stained and the dark areas are AuNPs. It can be seen that AuNPs are immobilized on the entire NFSKs. More interestingly, the AuNPs form Au lines on the NHSK, and the lines are perpendicular to the nanofiber. Within each line, the AuNPs are relatively closely packed across the entire fiber width. Furthermore, the Au lines are periodically located on the fiber, and the period is ~20 nm, which is consistent with the period of the HS-PEO NFSK in Figure 4. This remarkable observation suggests that immobilization of the AuNP on the NFSK is because of the formation of the Au−S bonds between HS-PEO and the AuNP, which can be further supported by a control experiment. In brief, we incubated the same AuNP sol with HO-terminated PEO (HO-PEO, M_n ~ 2K) NFSK following the same experimental procedure. No AuNPs were observed on NFSK.

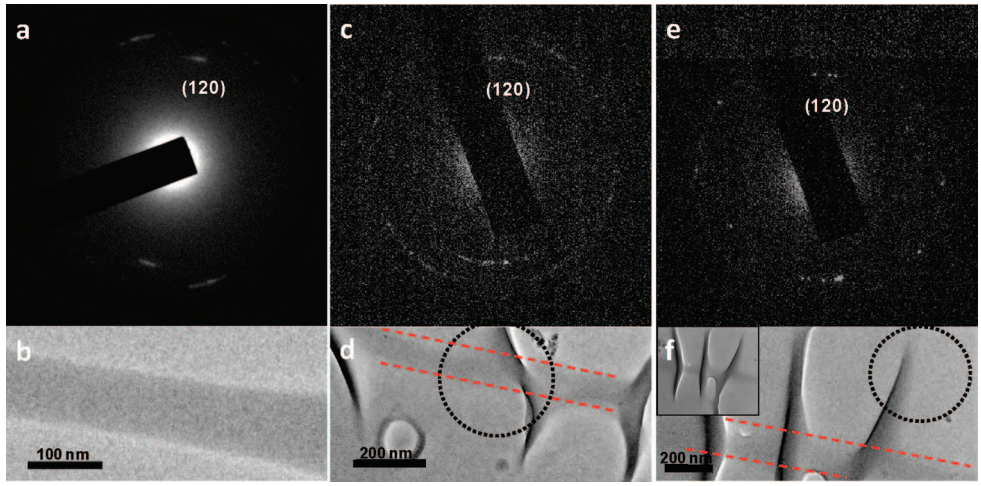

Figure 3. Electron diffraction patterns and the corresponding bright field TEM images of PEO nanofibers (a, b), NFSKs (c, d), and the kebabs (e, f). Note that platinum shading was not used. (120) diffraction can be clearly observed in all the three cases, suggesting a uniaxial orientation of the PEO chains in the fiber and the PEO chains in the kebabs are parallel to the fiber axis. In (d) and (f), the circles indicate the selected areas while the dotted lines indicate the fiber edges. The inset in (f) shows the entire NFSK.

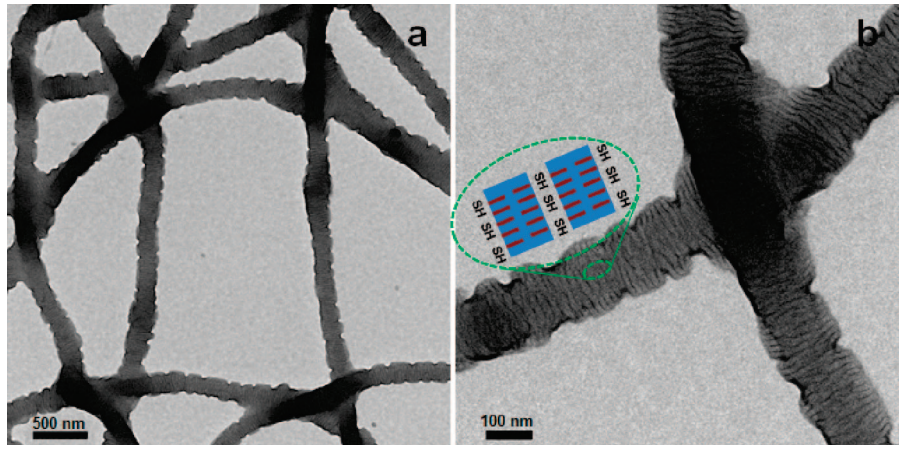

Figure 4. Low (a) and high (b) magnification TEM images of the NFSKs formed using HS-PEO as the K-P at a concentration of 2 wt %. The samples were stained with ruthenium tetroxide. The inset in (b) shows a schematic representation of the edge-on view of the PEO single crystals with a parallel packing scheme.

This clearly demonstrates that the HS functional groups are key to periodically patterning AuNPs on the nanofibers.

As previously discussed, the morphology of these NFSK nanofibers could be changed by tuning crystallization conditions. To this end, a different crystallization process was conducted where 5 μL of K−P/chloroform solution (2K HS-PEO with the concentration of 0.05 wt %) was drop-cast onto PEO nanofibers on a carbon-coated TEM grid and dried at room temperature. K-P crystallized during the solvent evaporation process, and the method was therefore referred to as a solvent evaporation approach. Similar NFSK structure was formed, and the kebab crystals in this process were formed within 1 min upon the evaporation of chloroform. AuNPs solution was used to incubate the NFSK nanofibers for 60 min. As a result, periodic alignment of AuNPs was obtained (Figures 5c,d) with the $\Lambda \sim 10$ nm, which is about half of the previous period (Figures 5a,b). It is intriguing that, by using the same S-P, K-P, and immobilization method, the Au line period changed by a factor of 2. This change suggests that the polymer chains packed differently during these two crystallization processes as shown in the insets of Figures 5b,d. 2K PEO crystallizes into an extended chain lamella where the entire polymer chain crystallizes without forming any folds, and the chain conformation is a 7_2 helix.[74,75] Since PEO chains are functionalized with HS groups at one end of the chain and methyl groups at the other, the ideal packing scheme in the HS-PEO single crystals is the parallel packing of the HS-PEO chains, leading to a bilayer structure. In this structure, HS groups aggregate on one surface of the crystal while the methyl groups pack on the other. For the incubation process (Figures 5a,b), the PEO chains had enough time to align themselves to achieve parallel packing during the crystallization process so that this bilayer structure was realized as shown in the inset of Figure 5b. However, in the case of crystallization process by solvent evaporation (Figures 5c,d), PEO chains did not have enough time to align themselves during the crystallization, and random head−tail orientation of the PEO chains was formed (single-layer packing). As a result, the thickness of kebabs decreased to about 10 nm, which is close to the extended chain length of 2K PEO (inset in Figure 5d). Note the pattern is also not as regular as that in Figures 5a,b, and some of the areas were not covered by AuNPs. This is also because of the poor packing of PEO chains during the fast solvent evaporation process. Therefore, because of the parallel and random packing of HS-PEO chains, the distances between adjacent HS layers are ~20 and 10 nm, respectively. This led to the difference of the AuNP line spacing. AuNP immobilization thus also served as a decoration method, revealing the subtle polymer chain packing during the crystallization process. Note that because the bilayer

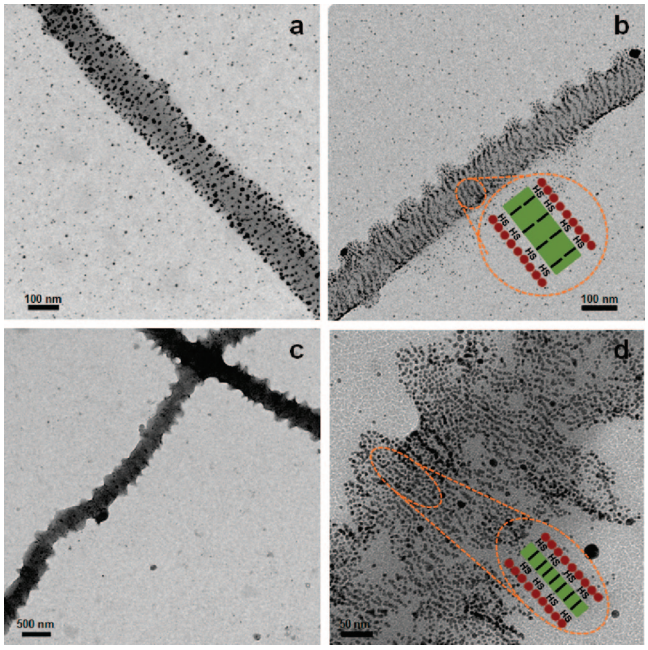

Figure 5. TEM images of AuNP-modified NFSKs using HS-PEO as the K-P. (a) and (b) were formed using the incubation crystallization method. The K-P concentration in (a) and (b) was 0.05 and 5 wt %, respectively. (c) and (d) were formed using the solvent evaporation method. (d) is an enlarged view of (c). Insets in (b) and (d) show the schematic representations of the edge-on view of the PEO crystals with a parallel or randomly packing scheme. Different packing schemes lead to the different periods in (b) and (d) (—: PEO chains; ●: AuNPs).

structure is more stable, it is possible to convert the single-layer to the bilayer packing by an extended annealing process. Nevertheless, because of the closely packed HS groups at the crystal surface, the single-layer packing perhaps is trapped in a deep well of the energy map (metastable state) and conversion to the bilayer structure might be difficult/slow. Different annealing processes are currently employed to study this conversion process.

Conclusions. Hierarchically ordered polymer nanofiber structure was obtained by combining electrospinning and controlled polymer crystallization methods. The unique nanoscale architecture, NFSK, resembles the conventional shish-kebab structure formed in polymers when crystallized under an extensional field. In the present case, the preformed nanofibers served as the shish and a secondary K-P was decorated on the nanofiber in the form of single crystal lamellae by either an incubation (slow crystallization) or a solvent evaporation (fast crystallization) method. The unique orthogonal orientation of the lamellae and the nanofiber was attributed to the soft epitaxy mechanism. This architecture is of great technological interest because it provides a platform for incorporating different functionalities into nanoscale polymer fibers in an ordered fashion. As a proof-of-concept, we immobilized AuNPs on the PEO nanofiber by using HS-PEO as the K-P. AuNPs formed regular lines, and these AuNP lines were periodically patterned on the PEO nanofiber. The period was controlled by tuning crystallization conditions. It is anticipated that this novel structure can find wide applications in the fields of sensors, catalyst support, nanoelectronics, and tissue engineering.

Acknowledgment. This work was supported by the National Science Foundation Grant DMR-0804838.

References and Notes

(1) Reneker, D. H.; Chun, I. *Nanotechnology* **1996**, *7*, 216–223.
(2) Dzenis, Y. *Science* **2004**, *304*, 1917–1919.
(3) Shin, Y. M.; Hohman, M. M.; Brenner, M. P.; Rutledge, G. C. *Polymer* **2001**, *42*, 9955–9967.
(4) Li, D.; Xia, Y. N. *Adv. Mater.* **2004**, *16*, 1151–1170.
(5) Greiner, A.; Wendorff, J. H. *Angew. Chem., Int. Ed.* **2007**, *46*, 5670–5703.
(6) Reneker, D. H.; Yarin, A. L. *Polymer* **2008**, *49*, 2387–2425.
(7) Fridrikh, S. V.; Yu, J. H.; Brenner, M. P.; Rutledge, G. C. *Phys. Rev. Lett.* **2003**, *90*, 144502.
(8) Chronakis, I. S. *J. Mater. Process. Technol.* **2005**, *167*, 283–293.
(9) Lin, T.; Wang, H. X.; Wang, X. G. *Adv. Mater.* **2005**, *17*, 2699–2703.
(10) Li, D.; Xia, Y. N. *Nano Lett.* **2004**, *4*, 933–938.
(11) Roh, K. H.; Martin, D. C.; Lahann, J. *Nat. Mater.* **2005**, *4*, 759–763.
(12) Sanders, E. H.; Kloefkorn, R.; Bowlin, G. L.; Simpson, D. G.; Wnek, G. E. *Macromolecules* **2003**, *36*, 3803–3805.
(13) Sun, Z. C.; Zussman, E.; Yarin, A. L.; Wendorff, J. H.; Greiner, A. *Adv. Mater.* **2003**, *15*, 1929–1932.
(14) Zhang, Y. Z.; Huang, Z. M.; Xu, X. J.; Lim, C. T.; Ramakrishna, S. *Chem. Mater.* **2004**, *16*, 3406–3409.
(15) Loscertales, I. G.; Barrero, A.; Marquez, M.; Spretz, R.; Velarde-Ortiz, R.; Larsen, G. *J. Am. Chem. Soc.* **2004**, *126*, 5376–5377.
(16) Li, D.; Wang, Y. L.; Xia, Y. N. *Adv. Mater.* **2004**, *16*, 361–366.
(17) Jiang, L.; Zhao, Y.; Zhai, J. *Angew. Chem., Int. Ed.* **2004**, *43*, 4338–4341.
(18) Acatay, K.; Simsek, E.; Ow-Yang, C.; Menceloglu, Y. Z. *Angew. Chem., Int. Ed.* **2004**, *43*, 5210–5213.
(19) Deitzel, J. M.; Kosik, W.; McKnight, S. H.; Tan, N. C. B.; DeSimone, J. M.; Crette, S. *Polymer* **2002**, *43*, 1025–1029.
(20) Bognitzki, M.; Czado, W.; Frese, T.; Schaper, A.; Hellwig, M.; Steinhart, M.; Greiner, A.; Wendorff, J. H. *Adv. Mater.* **2001**, *13*, 70–72.
(21) Megelski, S.; Stephens, J. S.; Chase, D. B.; Rabolt, J. F. *Macromolecules* **2002**, *35*, 8456–8466.
(22) Ruotsalainen, T.; Turku, J.; Heikkila, P.; Ruokolainen, J.; Nykanen, A.; Laitinen, T.; Torkkeli, M.; Serimaa, R.; ten Brinke, G.; Harlin, A.; Ikkala, O. *Adv. Mater.* **2005**, *17*, 1048–1052.
(23) Babel, A.; Li, D.; Xia, Y. N.; Jenekhe, S. A. *Macromolecules* **2005**, *38*, 4705–4711.
(24) Li, D.; Wang, Y. L.; Xia, Y. N. *Nano Lett.* **2003**, *3*, 1167–1171.
(25) Theron, A.; Zussman, E.; Yarin, A. L. *Nanotechnology* **2001**, *12*, 384–390.
(26) Dersch, R.; Liu, T. Q.; Schaper, A. K.; Greiner, A.; Wendorff, J. H. *J. Polym. Sci., Part A: Polym. Chem.* **2003**, *41*, 545–553.
(27) Kameoka, J.; Craighead, H. G. *Appl. Phys. Lett.* **2003**, *83*, 371–373.
(28) Chew, S. Y.; Wen, J.; Yim, E. K. F.; Leong, K. W. *Biomacromolecules* **2005**, *6*, 2017–2024.
(29) Luu, Y. K.; Kim, K.; Hsiao, B. S.; Chu, B.; Hadjiargyrou, M. *J. Controlled Release* **2003**, *89*, 341–353.
(30) Wang, X. Y.; Drew, C.; Lee, S. H.; Senecal, K. J.; Kumar, J.; Sarnuelson, L. A. *Nano Lett.* **2002**, *2*, 1273–1275.
(31) Bognitzki, M.; Becker, M.; Graeser, M.; Massa, W.; Wendorff, J. H.; Schaper, A.; Weber, D.; Beyer, A.; Golzhauser, A.; Greiner, A. *Adv. Mater.* **2006**, *18*, 2384–2386.
(32) Li, Z. Y.; Zhang, H. N.; Zheng, W.; Wang, W.; Huang, H. M.; Wang, C.; MacDiarmid, A. G.; Wei, Y. *J. Am. Chem. Soc.* **2008**, *130*, 5036–5037.
(33) Caruso, R. A.; Schattka, J. H.; Greiner, A. *Adv. Mater.* **2001**, *13*, 1577–1579.
(34) Han, G. Y.; Guo, B.; Zhang, L. W.; Yang, B. S. *Adv. Mater.* **2006**, *18*, 1709–1712.
(35) Patel, A. C.; Li, S. X.; Wang, C.; Zhang, W. J.; Wei, Y. *Chem. Mater.* **2007**, *19*, 1231–1238.
(36) Badami, A. S.; Kreke, M. R.; Thompson, M. S.; Riffle, J. S.; Goldstein, A. S. *Biomaterials* **2006**, *27*, 596–606.
(37) Li, M. Y.; Mondrinos, M. J.; Gandhi, M. R.; Ko, F. K.; Weiss, A. S.; Lelkes, P. I. *Biomaterials* **2005**, *26*, 5999–6008.
(38) Wnek, G. E.; Carr, M. E.; Simpson, D. G.; Bowlin, G. L. *Nano Lett.* **2003**, *3*, 213–216.
(39) Zong, X. H.; Kim, K.; Fang, D. F.; Ran, S. F.; Hsiao, B. S.; Chu, B. *Polymer* **2002**, *43*, 4403–4412.
(40) Kim, K.; Yu, M.; Zong, X. H.; Chiu, J.; Fang, D. F.; Seo, Y. S.; Hsiao, B. S.; Chu, B.; Hadjiargyrou, M. *Biomaterials* **2003**, *24*, 4977–4985.
(41) Liang, D.; Hsiao, B. S.; Chu, B. *Adv. Drug Delivery Rev.* **2007**, *59*, 1392–1412.
(42) Ko, F.; Gogotsi, Y.; Ali, A.; Naguib, N.; Ye, H. H.; Yang, G. L.; Li, C.; Willis, P. *Adv. Mater.* **2003**, *15*, 1161–1165.
(43) Larsen, G.; Velarde-Ortiz, R.; Minchow, K.; Barrero, A.; Loscertales, I. G. *J. Am. Chem. Soc.* **2003**, *125*, 1154–1155.

(44) Ge, J. J.; Hou, H. Q.; Li, Q.; Graham, M. J.; Greiner, A.; Reneker, D. H.; Harris, F. W.; Cheng, S. Z. D. *J. Am. Chem. Soc.* **2004**, *126*, 15754–15761.
(45) Demir, M. M.; Gulgun, M. A.; Menceloglu, Y. Z.; Erman, B.; Abramchuk, S. S.; Makhaeva, E. E.; Khokhlov, A. R.; Matveeva, V. G.; Sulman, M. G. *Macromolecules* **2004**, *37*, 1787–1792.
(46) Dai, H. Q.; Gong, J.; Kim, H.; Lee, D. *Nanotechnology* **2002**, *13*, 674–677.
(47) Li, D.; Xia, Y. N. *Nano Lett.* **2003**, *3*, 555–560.
(48) Ding, B.; Kim, H.; Kim, C.; Khil, M.; Park, S. *Nanotechnology* **2003**, *14*, 532–537.
(49) Hou, H. Q.; Reneker, D. H. *Adv. Mater.* **2004**, *16*, 69–73.
(50) Fong, H.; Reneker, D. H. *J. Polym. Sci., Part B: Polym. Phys.* **1999**, *37*, 3488–3493.
(51) Kalra, V.; Mendez, S.; Lee, J. H.; Nguyen, H.; Marquez, M.; Joo, Y. L. *Adv. Mater.* **2006**, *18*, 3299–3303.
(52) Ma, M. L.; Krikorian, V.; Yu, J. H.; Thomas, E. L.; Rutledge, G. C. *Nano Lett.* **2006**, *6*, 2969–2972.
(53) Ma, M. L.; Gupta, M.; Li, Z.; Zhai, L.; Gleason, K. K.; Cohen, R. E.; Rubner, M. F.; Rutledge, G. C. *Adv. Mater.* **2007**, *19*, 255–259.
(54) Ma, M. L.; Mao, Y.; Gupta, M.; Gleason, K. K.; Rutledge, G. C. *Macromolecules* **2005**, *38*, 9742–9748.
(55) Tuteja, A.; Choi, W.; Ma, M. L.; Mabry, J. M.; Mazzella, S. A.; Rutledge, G. C.; McKinley, G. H.; Cohen, R. E. *Science* **2007**, *318*, 1618–1622.
(56) Jana, N. R.; Peng, X. G. *J. Am. Chem. Soc.* **2003**, *125*, 14280–14281.
(57) Son, W. K.; Youk, J. H.; Lee, T. S.; Park, W. H. *Polymer* **2004**, *45*, 2959–2966.
(58) Li, C. Y.; Li, L. Y.; Cai, W. W.; Kodjie, S. L.; Tenneti, K. K. *Adv. Mater.* **2005**, *17*, 1198–1202.
(59) Li, L. Y.; Li, C. Y.; Ni, C. Y. *J. Am. Chem. Soc.* **2006**, *128*, 1692–1699.
(60) Li, L. Y.; Yang, Y.; Yang, G. L.; Chen, X. M.; Hsiao, B. S.; Chu, B.; Spanier, J. E.; Li, C. Y. *Nano Lett.* **2006**, *6*, 1007–1012.
(61) Kodjie, S. L.; Li, L.; Li, B.; Cai, W.; Li, C. Y.; Keating, M. *J. Macromol. Sci., Phys.* **2006**, *45*, 231–245.
(62) L. Li, L.; Li, C. Y.; Ni, C.; Rong, L.; Hsiao, B. S. *Polymer* **2007**, *48*, 3452–3460.
(63) Li, L.; Li, B.; Yang, G.; Li, C. Y. *Langmuir* **2007**, *23*, 8522–8525.
(64) Ning, N. Y.; Luo, F.; Pan, B. F.; Zhang, Q.; Wang, K.; Fu, Q. *Macromolecules* **2007**, *40*, 8533–8536.
(65) Uehara, H.; Kato, K.; Kakiage, M.; Yamanobe, T.; Komoto, T. *J. Phys. Chem. C* **2007**, *111*, 18950–18957.
(66) Zhang, Z. W.; Xu, Q.; Chen, Z. M.; Yue, J. *Macromolecules* **2008**, *41*, 2868–2873.
(67) Geil, P. *Polymer Single Crystals*; Robert Krieger Pub.: Huntington, NY, 1973.
(68) Birnkrant, M. J.; McWilliams, H.; Li, C. Y.; Natarajan, L.; Tondiglia, V. P.; Lloyd, P. F.; Sutherland, R. L.; Bunning, T. J. *Polymer* **2006**, *47*, 8147–8154.
(69) Birnkrant, M. J.; Li, C. Y.; Natarajan, L.; Tondiglia, V. P.; Lloyd, P. F.; Sutherland, R. L.; Bunning, T. J. *Nano Lett.* **2007**, *7*, 3128–3133.
(70) Li, D.; McCann, J. T.; Gratt, M.; Xia, Y. N. *Chem. Phys. Lett.* **2004**, *394*, 387–391.
(71) Li, B.; Li, C. Y. *J. Am. Chem. Soc.* **2007**, *129*, 12–13.
(72) Li, B.; Ni, C.; Li, C. Y. *Macromolecules* **2008**, *41*, 149–155.
(73) Wang, B. B.; Li, B.; Zhao, B.; Li, C. Y. *J. Am. Chem. Soc.* **2008**, *130*, 11594-11595.
(74) Kovacs, A. J.; Straupe, C. *J. Polym. Sci., Polym. Symp.* **1977**, *59*, 31–54.
(75) Cheng, S. Z. D.; Chen, J. H.; Barley, J. S.; Zhang, A. Q.; Habenschuss, A.; Zschack, P. R. *Macromolecules* **1992**, *25*, 1453–1460.

MA801971R